MDOX where twist does not play a role, MM2 predicts a difference of 2.0 kcal/mol between equatorial and axial which is consistent with the ED result where only equatorial was observed.

For MDOX equatorial is the only conformation found in substantial quantity. MM2 calculations seem to suggest twist is neither a minimum nor a maximum on the pseudorotational trajectory. Equatorial is definitely the lowest energy form in agreement with the experiment. We believe that due to the repulsive forces of the methyl group, axial might very well be a maximum on the potential surface. Thus the pseudorotation of MDOX is governed by a onefold function with high barrier at axial and minimum at equatorial. For DMDOX a dynamic model with a twofold potential function fit the ED data very admirably, and the barrier was found to be 1.1 ± 0.3 kcal/mol.

It is very likely that the barrier in DOX is less than 1.1 kcal/mol (the barrier obtained for DMDOX) because with the absence of the two bulky methyl groups the pseudorotation in DOX should be less hindered. In summary, this study suggests that DOX has a very low barrier to pseudorotation with twist as the minimum; MDOX can be described by using a onefold potential with equatorial as the minimum, and DMDOX has a twofold barrier of 1.1 kcal/mol with twist as the minimum energy conformer.

At the conclusion of this research we became aware of the fact that Professor Kenneth Hedberg, Department of Chemistry, Oregon State University, had also recently completed a gas phase electron diffraction study of DOX. We have compared our results with those of Professor Hedberg, and we find no significant differences in any of the reported structural parameters.

Acknowledgment. We are grateful to the financial support provided by the National Science Foundation (Grant No. 8111739).

Registry No. DOX, 646-06-0; MDOX, 497-26-7; DMDOX, 2916-31-6.

Supplementary Material Available: Tables of correlation matrixes and intensity data (12 pages). Ordering information is available on any current masthead page.

Oscillations and Bistability in the Cu(II)-Catalyzed Reaction between H_2O_2 and KSCN

Miklós Orbán

Contribution from the Institute of Inorganic and Analytical Chemistry, L. Eötvös University, Budapest H-1443, Hungary. *Received April 28, 1986*

Abstract: The reaction between H_2O_2 and KSCN catalyzed by $CuSO_4$ exhibits three different types of bistability as a function of flow rate in a continuous flow stirred tank reactor at 25 °C. Two steady states and one oscillatory state are involved. The system is one of the few examples in which oscillations can appear in batch configuration as well. The color, the potential of a Pt electrode, and the rate of oxygen gas evolution oscillate for a wide range of reagent concentrations. The chemistry which accounts for the observed behavior is discussed briefly.

The rapidly growing interest in and number of examples of oscillatory and related phenomena suggest that chemical oscillations and multistability are a frequent rather than an exceptional form of behavior in far-from-equilibrium systems. It is still a problem to find the proper conditions under which these phenomena can occur. Mathematical models are capable of predicting these behaviors from solutions to the appropriate differential equations, although wide gaps still exist between the models and the real chemical systems. A few authors claim that an oscillatory chemical reaction can be constructed by design. It is perhaps fairer to say that until now only some general requirements have been established (e.g., far-from-equilibrium conditons, feedback, nonlinear kinetics, etc.) which may result in oscillations under certain combinations of the constraints. A semiempirical approach of constructing oscillatory chemical systems was successfully applied in recent years, and the technique coupled with a little luck, and fantasy has led to the discovery of dozens of new oscillators.[1] In spite of the large number of examples, only a few are based on really different chemistry, whereas the majority represent variations with more or less essential modifications of the so-called "minimal" versions. An effort to classify the known liquid-phase chemical oscillators was made in a recently published monograph[2] in which three basic groups were distinguished: the classes of iodate, bromate, and chlorite oscillators.

Some very recent results have shown that species other than oxyhalogens can also give rise to oscillations, bistability, and excitability in solution. Examples are the oxidation of benzaldehyde by oxygen in glacial acetic acid with $CoBr_2$ catalyst,[3] the oxidation of methylene blue by oxygen in strongly alkaline medium in the presence of sulfite and sulfide,[4] and the oxidation of sulfide ion with hydrogen peroxide in nearly neutral solution.[5] In the H_2O_2–S^{2-} reaction, among other periodic responses, pH oscillations of some 3–4 units were observed.

The new oscillatory reaction reported in this paper may represent a member of a fundamentally new group. It has an initial composition of KSCN–H_2O_2–$CuSO_4$–NaOH; it shows several types of bistability; it oscillates in color, in potential of a Pt electrode and in the rate of gas evolution; but it gives no pH oscillations. For the oscillation, the pH must be above 9 and the periodicity appears in both batch and flow configurations.

Experimental Section

Materials. Stock solutions of KSCN and NaOH were prepared using analytical grade chemicals dissolved in distilled water previously passed through an ion-exchange column filled with oxycellulose to remove any trace metal impurities. After this treatment of the water, atomic absorption spectrophotometry indicated no measurable amount of metal ion contamination. The concentrations of KSCN and NaOH were checked by the Volhard and acid–base titration methods, respectively. The H_2O_2 solutions were always freshly made by dilution of commercially available Fisher Certified ACS 30% or Reanal 30% product, and kept in poly-

(1) Epstein, I. R.; Kustin, K.; De Kepper, P.; Orbán, M. *Sci. Am.* **1983**, *248*, (3), 112–123.
(2) Epstein, I. R.; Orbán, M. *Oscillations and Traveling Waves in Chemical Systems*; Field, R. J., Burger, M., Eds.; Wiley: New York, 1984; Chapter 8, pp 257–286.
(3) Jensen, J. H. *J. Am. Soc.* **1983**, *105*, 2639–2641.
(4) Burger, M.; Field, R. J. *Nature (London)* **1984**, *307*, 720–721.
(5) Orbán, M.; Epstein, I. R. *J. Am. Chem. Soc.* **1985**, *107*, 2302–2305.

0002-7863/86/1508-6893$01.50/0

ethylene bottles to avoid decomposition. The stock solutions of H_2O_2 were titrated with standard $KMnO_4$. The $CuSO_4$ stock solution was prepared and stored in slightly acidic medium (4×10^{-3} M/dm^3 $CuSO_4 \cdot 5H_2O$ in pH ~4 H_2SO_4 solution) to prevent hydrolysis during storage. The required dilutions were made with distilled water.

Apparatus and Methods. In the *batch* experiments the components in appropriate concentrations were mixed in the reaction vessel, and visual and instrumental observations were made until changes in the responses occurred. The reactor was thermostated at 25.00 ± 0.05 °C and equipped with a magnetic stirrer and Pt and pH sensors. The platinum electrode (Radiometer P 101) together with a $Hg|Hg_2SO_4|K_2SO_4$ reference electrode (Radiometer K 601) were directly connected to a double channel chart recorder (Kipp & Zonen BD-9). The combined glass electrode (Metrohm EA 120) was attached to the same recorder (through a Radelkis OP-208 digital pH meter) which allowed us to record simultaneous changes of the redox potential and pH. The optical density during the reaction was measured by a double beam recording spectrophotometer (Specord UV VIS Zeiss) using 2-cm-long cells. The mixing in the cell was ensured by introducing high-purity nitrogen into the cell through a capillary tube which produced a bubble-free but efficient convection in the part of the soltuion where the light beam passed through the cell. The gaseous product of the reaction was analyzed with a mass spectrometer (Balzers QMS 101 with peak selector) using a specially designed cell. An intense argon stream purged the gas product from the reaction mixture and carried it into the mass spectrometer. The product gas was analyzed for H_2 and O_2 and their production rate was monitored. Some polarographic recordings at constant potential (−0.6 V vs. SCE) were also made (PO 4 Radiometer, Copenhagen; Bruckner dropping Hg electrode) to follow the rate of oxygen evolution in the reaction mixture during the oscillations.

The KSCN–H_2O_2–Cu(II) system has been studied under *flow* condition as well. The CSTR (continuous flow stirred tank reactor) had a volume of 30.2 cm^3 and operated in isothermal mode at 25.00 ± 0.05 °C. The reactor was fed by a Sage 375 A peristaltic pump through four inlet tubes, and the outflow was connected to an aspirator. All solutions were stirred magnetically at 600 rpm. The design of the reactor precluded any air gap between the surface of the reaction mixture and the reactor cap. In flow configuration only two signals, the potential of Pt electrode and that of pH electrode, were recorded.

In order to search for multistability or oscillations, the following experimental technique was applied. The reactor was filled with the prethermostated input solutions at the highest available pump speed, and this flow was maintained until a steady state was attained. With a stepwise decrease of the flow rate to zero, the flow branch of the response-flow rate diagram is established by recording the steady or oscillatory states reached in the reactor after each step. When the sequence of steady states is monitored by increasing the flow stepwise from zero to high values, we can plot the thermodynamic branch of the response-flow rate phase diagram. The range of these two branches is mainly determined by the constraints applied in the experiments. In some cases, however, we encounter hysteresis in the two-direction responses which indicates that two (or more) states can exist under the same constraints, i.e., the system is bistable (or multistable) in certain regions of the variables. The state which is found depends on the direction from which the state was approached, and reversible transitions between the states may be induced by appropriate perturbations. In a bistable situation two steady states, or one steady state and one oscillatory state, or two oscillatory states can be involved.

Results

Batch. When a KSCN solution is mixed with excess H_2O_2 at high pH (pH ≥9) no visible change is observed. However, Pt and glass electrodes immersed in the mixture indicate that an oxidation process with moderate rate occurs in which the potential of the Pt electrode increases and the pH slowly decreases (see Figure 1, curves a and b). If a catalytic amount of Cu(II) ion is added to the initial reaction mixture, it turns an intense yellow color. The rate of the reaction (i.e., the slopes of the Pt and pH traces) does not seem to change dramatically, but pronounced oscillations appear on the Pt potential superimposed on the smooth line measured during the Cu(II)-free KSCN–H_2O_2 reaction (Figure 1, curves a′ and b′). The process is also accompanied by oscillations in color between dark yellow and pale yellow or colorless. When the Pt potential drops to its minimum, the color fades gradually. The pH does not show oscillations, but at low initial NaOH concentrations (pH <8.5) a stepwise decrease in pH (~0.1 pH unit) was observed as the reaction proceeded. The experimental results are depicted in Figure 2, which represents on the same time scale the changes in optical density, in the potential of a Pt electrode, in pH, and in the rate of oxygen gas evolution measured with a mass spectrometer. We do not show the polarographic oxygen vs. time recording because it is essentially identical with curve d of Figure 2.

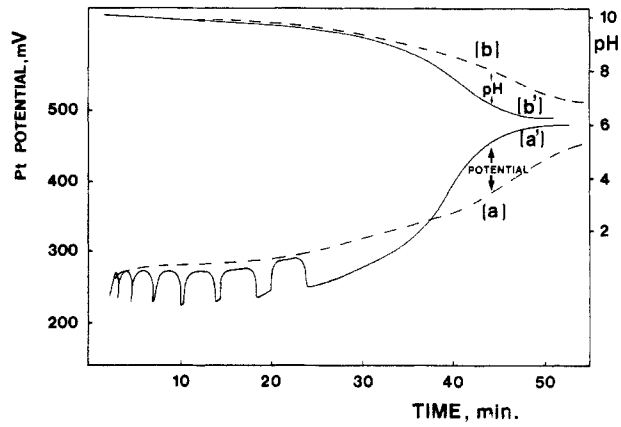

Figure 1. The potential of Pt electrode (curves a and a′) and pH (curves b and b′) vs. time in the reaction between H_2O_2 and KSCN in alkaline solution with (solid line) and without (dotted line) Cu(II) ion catalyst. The initial concentrations (M) are: $[H_2O_2]_0$, 0.25,; $[KSCN]_0$, 0.025; $[NaOH]_0$, 0.025, $[CuSO_4]_0$, 7.5×10^{-5} (temp 25 °C).

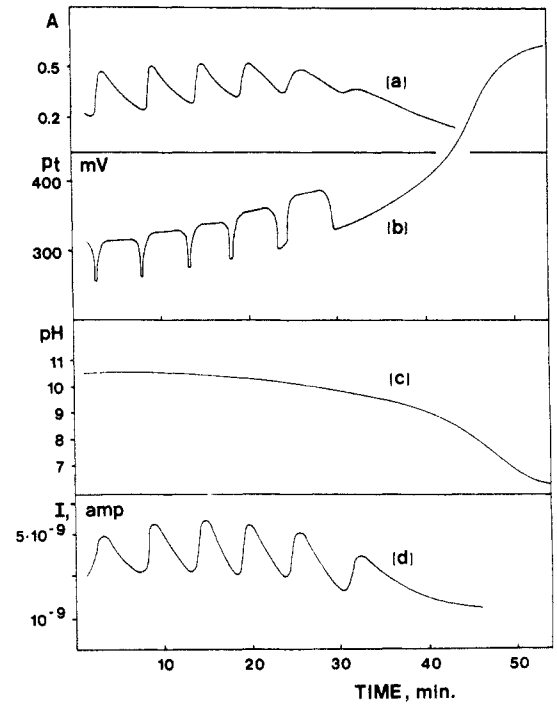

Figure 2. The different responses vs. time in the oscillatory Cu(II)-catalyzed reaction between H_2O_2 and KSCN. The initial concentrations (M) are: $[H_2O_2]_0$, 0.25; $[KSCN]_0$, 0.0375; $[NaOH]_0$, 0.025; $[CuSO_4]_0$, 7.5×10^{-5} (temp 25 °C). Curves: (a) absorbance at 375 nm, cell width 2 cm; (b) potential of Pt electrode against $Hg|Hg_2SO_4|K_2SO_4$ reference electrode; (c) pH; (d) ionic current in amperes recorded with mass spectrometer for the species of mass number 32. The ionic current is proportional to the amount of oxygen evolved in and driven out of the reaction mixture.

In both our batch and flow experiments the following ranges of concentrations (M) were tested: $[H_2O_2]$, 0.1–0.5; [KSCN], 0.005–0.1; [NaOH], 0.001–0.1; $[CuSO_4]$, 5×10^{-5}–2×10^{-4} (at concentrations above 2×10^{-4} M visible precipitation of a brownish Cu compound occurs). The trends in the effect of concentration on the behavior of the system are illustrated in Figure 3. The figure shows the changes in number, amplitude, and frequency of the oscillations when one of the reactant concentrations is doubled compared to the composition of the oscillatory curve a′ of Figure 1. The increase of both H_2O_2 and KSCN concentrations

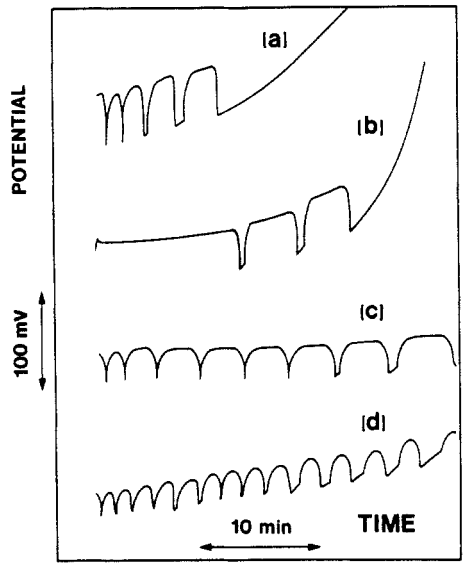

Figure 3. Dependence of the oscillation frequency and amplitude on reagent concentration and potential of Pt electrode vs. time traces in batch. For comparison see Figure 1, curve a'. The following changes in composition were made: (a) $[H_2O_2]_0$, 0.5 M; (b) $[KSCN]_0$, 0.05 M; (c) $NaOH]_0$, 0.05 M, (d) $[CuSO_4]_0$, 1.5×10^{-4} M.

speeds up the reaction and more pronounced but fewer oscillations appear. Increased catalyst concentration and pH seem to be more favorable for the oscillations.

The KSCN and NaOH cannot be replaced with NH_4SCN and NH_4OH, respectively, because the NH_4^+ (or NH_3) proved to be an inhibitor of the oscillations. This is striking because NH_4^+ is an end product of the reaction between H_2O_2 and KSCN (see eq 1 and 2). Adding 0.05 M NH_4OH to the oscillatory composition of Figure 1a' or establishing the initial pH by using NH_4OH gives a curve like that shown in Figure 1a. Complex-forming compounds, like EDTA, have the same effect in much smaller concentrations ($\sim 10^{-4}$ M). The CN^- ion, known to form a very stable complex with copper ion, does not suppress oscillations even at 10^{-2} M. These observations suggest that ligands resistant to H_2O_2 oxidation like NH_3 or EDTA can poison the catalyst owing to complex formation. The CN^- is an intermediate in the H_2O_2–KSCN reaction and undergoes oxidation rather than giving rise to a complex with copper ion.

Efforts were made to replace the Cu(II) catalyst with metal ions of similar chemical properties such as Ag(I) and Hg(II) ions. No oscillations were observed in the presence of these and other metal ions like Fe(II), Co(II), and Ni(II), which are known catalysts for the decomposition of H_2O_2. The Cu(II) ion is concluded to be a unique species capable of bringing about oscillations in the alkaline H_2O_2–KSCN system.

Flow. Under flow conditions in CSTR the damped oscillations presented in Figures 1–3 become sustained. The initial concentrations for oscillations, however, are not always identical in batch and flow. At some compositions, mainly at low KSCN (e.g., 0.005–0.008 M KSCN and 0.25 M H_2O_2, 0.01–0.02 M NaOH, 5×10^{-5} M Cu(II)), the system shows oscillations only at zero flow rate (i.e., in batch) and a steady state appears in flow. The amplitude and frequency of the oscillations are functions of the initial reagent concentrations, similar to what is shown in Figure 3, and of the flow rate. In Figure 4 some oscillatory traces of the Pt potential are presented at different flow rates.

The oscillations occur in a wide range of concentrations and flow rates. The ranges extend to nearly two orders of magnitude in the concentrations and to an order of magnitude in the flow rates. Besides the oscillations, two steady states and different bistabilities between them can be established in the H_2O_2–KSCN–NaOH–Cu(II) flow system by variations of the flow rate and input concentrations. Steady-state I (SS I) is associated with a low Pt potential (200–400 mV) and high pH (8–11) which suggest a small extent of reaction between H_2O_2

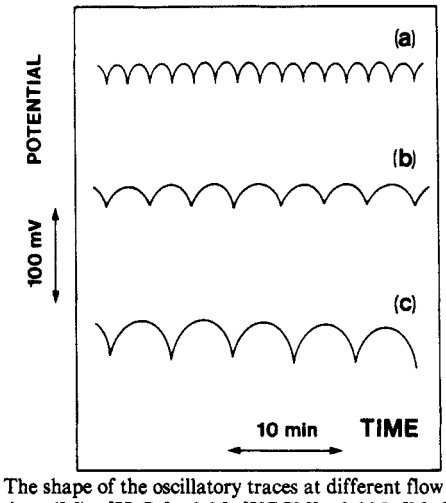

Figure 4. The shape of the oscillatory traces at different flow rates. Input concentrations (M): $[H_2O_2]_0$, 0.25; $[KSCN]_0$, 0.025; $[NaOH]_0$, 0.025; $[Cu(II)]_0$, 5×10^{-5}. Flow rates (s^{-1}): (a) 8.1×10^{-3}, (b) 2.7×10^{-3}, (c) 1.0×10^{-3}. Temperature 25 °C.

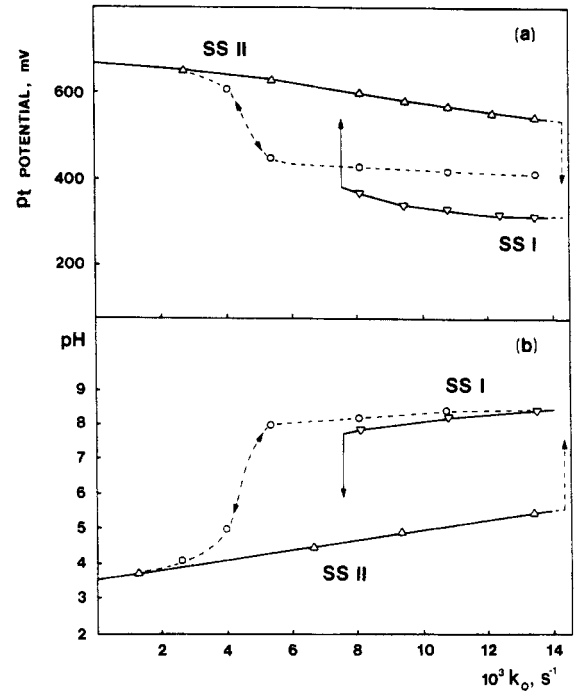

Figure 5. Hysteresis between SS I and SS II in the CSTR with input concentrations (M): $[H_2O_2]_0$, 0.25; $[KSCN]_0$, 0.025; $[NaOH]_0$, 0.001; $[CuSO_4]_0$, 5×10^{-5}: (a) potential of Pt electrode vs. flow rate; (b) pH vs. flow rate (temp 25 °C). For explanation of dotted lines see the text.

and KSCN. This steady state appears at lower KSCN and H_2O_2 concentrations, at high input NaOH, and at high flow rates. Steady-state II (SS II) can be observed under experimental conditions where high conversion is possible, i.e., at high KSCN and H_2O_2 concentrations, at low input NaOH, and at lower flow rates. The prevailing stoichiometry here can probably be approximated by eq 1 and/or 2. SS II is associated with a higher Pt potential (500–700 mV) and a lower pH (3–5). A difference in color exists between the two steady states; SS I is colorless and SS II is yellowish

In the H_2O_2–KSCN–NaOH–$CuSO_4$ system we encounter three different bistabilities under flow conditions in which the following combinations of states are involved: (i) SS I ↔ SS II; (ii) oscillatory state ↔ SS II; (iii) SS I ↔ oscillatory state.

Bistability between SS I and SS II is illustrated by the hysteresis curves in the Pt potential and pH on variation of the flow rate at fixed input concentrations in Figure 5, curves a and b, respectively. Starting from the high-flow-rate side in Figure 5 curves a and b, the flow branch (SS I) of the response–flow rate diagram is established until k_0 reaches 7.5×10^{-3} s^{-1}. Upon further de-

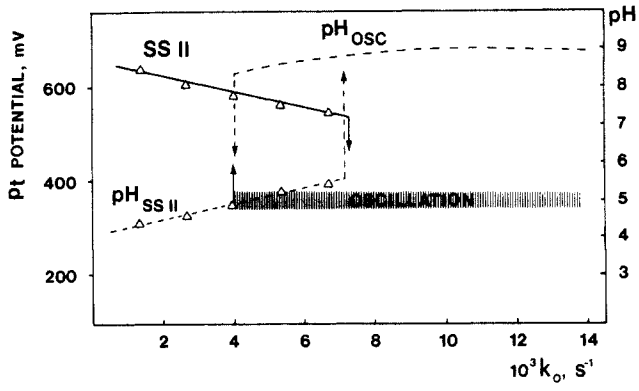

Figure 6. Hysteresis between SS II and the oscillatory state in the potential of Pt vs. flow rate plane. For explanation of dotted lines see text. Input concentrations (M): $[H_2O_2]_0$, 0.25; $[KSCN]_0$, 0.025, $[NaOH]_0$, 0.002; $[CuSO_4]_0$, 5×10^{-5}.

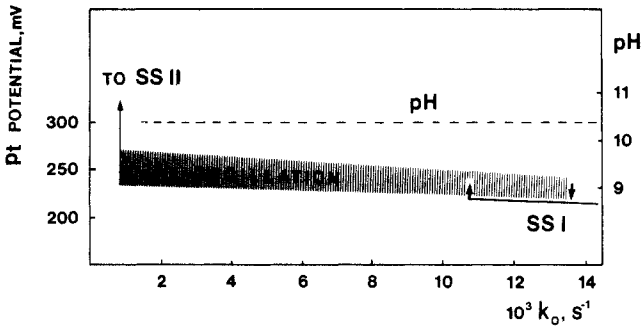

Figure 7. Hysteresis between the oscillatory state and SS I in the potential of Pt vs. flow rate plane. The conditions are as in Figure 6 with exception of the input NaOH concentration: $[NaOH]_0$ 0.025 M.

creasing the flow rate, a sharp transition to SS II occurs. The color changes from colorless to yellow, the potential jumps up, and the pH drops and stays on the SS II curve as the flow is decreased further. Starting from $k_0 = 0$ and increasing the flow toward higher values, we are on the thermodynamic branch SS II. The reverse transition from SS II to SS I happens at a higher flow rate than is achievable with our pump, which indicates a broad range of bistability. The transition here can be reached by perturbation, e.g., by transient NaOH additon. The dotted lines in Figure 5a,b present the responses when the copper catalyst was omitted from the flow. The potential and pH values do not differ dramatically in the catalyst-containing and catalyst-free reaction mixtures at the two extreme flow rates, but without Cu(II), the responses of the system change smoothly in both directions along the dotted lines, indicating no hysteresis. The Cu(II) ion seems to be essential for the bistable behavior.

In the other two types of bistability the oscillatory state and one of the two steady states, SS I or SS II, are involved. These cases are illustrated in Figures 6 and 7. The diagrams were taken at two different input NaOH concentrations with all other constraints kept constant, and the states (potential and pH values) were determined on variation of the flow rates. As can be seen in Figure 6, for $k_0 \leq 4 \times 10^{-3}$ s^{-1} only SS II, at 4×10^{-3} s$^{-1} \leq k_0 \leq 7.2 \times 10^{-3}$ s^{-1} bistability between SS II and oscillations, and, at $k_0 \geq 7.2 \times 10^{-3}$ s^{-1}, only the oscillatory state appear in the Pt potential vs. flow rate phase plane under the conditions indicated in the figure caption. The vertical segments of the oscillatory striped area give the amplitude of the potential oscillations. The dotted lines in the figure show the hysteresis in the pH during the same process. In contrast with the Pt responses the pH curves have a steady-state character on both branches. High pHs belong to the oscillatory state and low pH accompanies SS II.

The bistability shown in Figure 7 has different features. In the Pt potential vs. flow rate plane, the oscillatory state and the other steady state (SS I) are involved in the hysteresis. The essential difference here compared to the previous case is that no hysteresis is observed in the pH. The pH stays at a high (pH

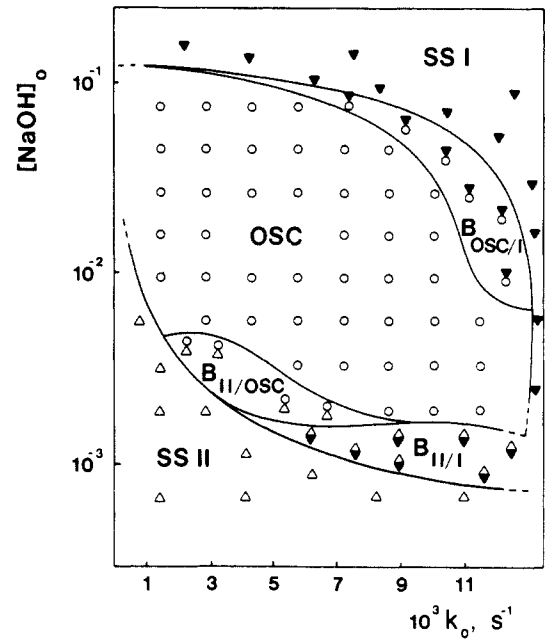

Figure 8. Phase diagram for the H_2O_2–KSCN–NaOH–$CuSO_4$ system in the $[NaOH]_0$–k_0 plane. Fixed constraints: $[H_2O_2]_0$, 0.25 M; $[KSCN]_0$, 0.025 M; $[CuSO_4]_0$, 5×10^{-5} M; temp 25 °C. Symbols: ▼, SS I; △, SS II; ○, oscillations. Combinations of the above symbols imply multistability among the corresponding modes.

~10.5) value at any flow rate regardless of the transitions in the Pt potential at $k_0 = 1.07 \times 10^{-2}$ and 1.36×10^{-2} s^{-1}. It is of interest that the oscillatory state appears as flow branch in Figure 6, whereas it represents the thermodynamic branch in Figure 7.

The possible states in a complex dynamical system and the relations between them may conveniently be displayed in a constraint–constraint phase diagram. In Figure 8 the boundary lines and ranges of the oscillations, steady states, and different bistabilities are presented in the input NaOH concentration vs. flow rate phase diagram at fixed input H_2O_2, KSCN, and $CuSO_4$ concentrations and temperature. The choice of $[NaOH]_0$ as the variable with all the other reagent concentrations constant is an arbitrary one, but in our multidimensional system the initial pH of the reaction mixture proved to be one of the most influential factors in determining the state attained by the system. Note that the response–constraint plots of Figures 5, 6, and 7 are included as three horizontal sections in the constraint–constraint phase diagram of Figure 8.

Discussion

The reaction between H_2O_2 and KSCN was first studied about 60 years ago[6] because it offered an analytical method for the quantitative determination of SCN^- through the NH_3 produced in the course of the alkaline oxidation of SCN^- by H_2O_2. The mechanism of the reaction was worked out by Wilson and Harris[7] and by Csányi and Horváth.[8] The reaction takes place according to slightly different mechanisms depending on the acidity of the solution. The reaction at pH <4 is catalyzed by $[H^+]$, but its rate is independent of the hydrogen ion concentration in the range 4 < pH < 12. The main acid-catalyzed process has the stoichiometry of eq 1 while the non-acid-catalyzed reaction obeys eq 2:

$$3H_2O_2 + SCN^- \rightarrow HSO_4^- + HCN + 2H_2O \quad (1)$$

$$4H_2O_2 + SCN^- \rightarrow HSO_4^- + NH_4^+ + HCO_3^- + H_2O \quad (2)$$

The reaction is first order in each reactant. The rate-determining step for both stoichiometries is

(6) Schuster, F. *Z. Anorg. Allg. Chem.* **1930**, *186*, 253–256.
(7) Wilson, I. R.; Harris, G. M. *J. Am. Chem. Soc.* **1960**, *82*, 4515–4517; **1961**, *83*, 286–289.
(8) Csányi, L. J.; Horváth, G. *Acta Chim. Hung.* **1962**, *34*, 1–6.

$$H_2O_2 + SCN^- \rightarrow HOSCN + OH^- \quad (3)$$

The species HOSCN is proposed for the product step 3 because of the known chemical similrity between SCN^- and halide ions (X^-) and the fact that HOX is the first product in the H_2O_2–X^- reactions.[9] Step 3 is followed in the mechanism by a series of fast oxidation and/or hydrolysis reactions in which HOOSCN, HSO_3^-, HCN, HOCN, and other intermediates are involved leading to the products in eq 1 and 2. Traces of Ni(II), Rh(III), and Fe(II) are stated to have no effect on the rate, although larger concentrations of ferrous salt caused some acceleration.[7] No study has been carried out so far when Cu(II) ion was employed as catalyst in the reaction between H_2O_2 and KSCN.

From Figure 1 one can see that in alkaline solution the added Cu(II) influences the system in two ways: (i) it makes the first part of the potential trace oscillatory; and (ii) it speeds up the reaction in the second stage causing a sigmoidal shape of the potential and pH responses.

It is well-known that Cu(II) ion readily reacts with both reagents. With SCN^- it forms a green complex $Cu(SCN)_4^{2-}$, which in the presence of reducing agents turns to white CuSCN precipitate, but the complex transforms to a bluish $Cu(OH)_2$ precipitate when the pH is in the alkaline region. It is also known that the catalytic decomposition of H_2O_2 is triggered by many metal ions, among them copper.[10] While the mechanism of the decomposition of H_2O_2 in the presence of Fe^{2+} and Fe^{3+}–Cu^{2+} mixtures in homogeneous (pH <3) solution is described in detail by Barb et al.,[11] and a generalization of the mechanism for bivalent metal ions has been constructed,[12] understanding of the copper ion catalyzed decomposition of H_2O_2 in alkaline solutions where the copper is initially present as colloidal $Cu(OH)_2$ is very limited.[13] At equimolar ratio or moderate excess of H_2O_2 to $Cu(OH)_2$ they react with formation of a brown copper(II) peroxide with a probable composition of Cu[OH][OOH]. At high excess H_2O_2, copper(II) peroxide in alkaline solution (pH 8–12) is reduced to a yellow diamagnetic copper(I) compound, which was proved by the disappearance of the ESR signal detected in the copper(II) peroxide.[14] The yellow compound is probably copper(I) peroxide. This compound appears immediately if we start with a high (>100) molar ratio of H_2O_2 to Cu(II) ion in a pH >8 solution.

The copper(II) and copper(I) peroxides are thought to be involved in the alkaline oxidation of H_2O_2 to O_2 via $HO_2^\bullet$ and $OH^\bullet$ radicals. An ESR study[14] also showed evidence of O_2^- radical, which is probably a precursor of O_2 evolution in the H_2O_2 decomposition.

Glaser[15] measured the absorbance at 470 nm due to copper(II) peroxide in parallel with the evolution of oxygen in the alkaline Cu(II)–H_2O_2 mixture. He found bell-shaped absorbance vs. time and S-shaped oxygen vs. time curves, and coincidence between the maximum absorbance and the steepest part of the S-shaped curve was established. In our experiments under oscillatory conditions, the maximum color intensity and a burst of O_2 evolution also coincided as shown in Figure 2, curves a and d. The visible spectrum of the oscillatory mixture, however, indicated a strong absorption at 375 nm due to a copper(I) compound and showed practically no copper(II) peroxide present. A yellow copper(III) compound (Cu(OH)O) was postulated to form in the interaction of Cu(I) and H_2O_2 at pH ~3 by Cahill and Taube,[16] but ESR measurements have not supported the presence of Cu(III) in a strongly alkaline H_2O_2 solution.[14] The conclusion can be drawn that in the color oscillations a copper(I) intermediate (most likely CuOOH) is the catalytically active species, and its reversible formation and decomposition result in the periodicity during the Cu(II)-catalyzed reaction between H_2O_2 and KSCN at pH >9.

In spite of some knowledge about the chemistry of the subsystems H_2O_2–KSCN, Cu^{2+}–SCN^- and $Cu(OH)_2$–H_2O_2, at the present time we are not able to give a full mechanistic explanation of the oscillation and bistabilities observed in the total system. Rough ideas about the origin of the phenomena may be the following. Since the copper ion free H_2O_2–KSCN system shows no bistability and the copper ion catalyzed reaction does, interactions between the intermediates of the subsystems must occur which autocatalytically accelerate the oxidation of SCN^- to H_2SO_4. The flow branch (SS I) in the bistable situation shown in Figures 5 and 7 may represent an early stationary stage due to a slow reaction, and the thermodynamic branch (SS II) in Figures 5 and 6 can be close to the stationary composition approximated by eq 1 and/or 2. The oscillations in the present system are due mainly to the chemistry which is responsible for the $Cu(OH)_2$-catalyzed autocalytic decomposition of H_2O_2. We can write the cycle schematically as:

$$2Cu^{2+} + 2OH^- + H_2O_2 \rightarrow 2Cu^+ + O_2 + 2H_2O \quad (4)$$

$$2Cu^+ + H_2O_2 \rightarrow 2Cu^{2+} + 2\,OH^- \quad (5)$$

The chain carriers in eq 4 and 5 are $HO_2^\bullet$, $HO^\bullet$, and Cu^+ according to eq 4a, 4b, 5a, and 5b.

$$Cu^{2+} + HOO^- \rightarrow Cu^+ + HO_2^\bullet \quad (4a)$$

$$Cu^{2+} + HO_2^\bullet \rightarrow Cu^+ + H^+ + O_2 \quad (4b)$$

$$Cu^+ + H_2O_2 \rightarrow Cu^{2+} + OH^- + HO^\bullet \quad (5a)$$

$$Cu^+ + HO^\bullet \rightarrow Cu^{2+} + OH^- \quad (5b)$$

Equations 4 and 5 yield eq 6, the Cu-catalyzed decomposition of H_2O_2.

$$2H_2O_2 \rightarrow 2H_2O + O_2 \quad (6)$$

The SCN^-, a known analytical reagent for Cu^+, has the role of separating in time the steps in which copper(I) forms and is temporarily stabilized by SCN^-; it is then reoxidized to the bivalent state with the simultaneous oxidation of the SCN^-. The interaction between copper(I) and SCN^- may result in a colloidal CuSCN precipitate. Some other colloidal species such as $Cu(OH)_2$, CuOH and copper peroxide can also be formed, and their periodic formation and dissolution may need to be considered in the kinetics responsible for the oscillations.

The elementary steps most likely involved in the oscillatory cycle are being collected, and a detailed mechanism is under construction and will be published in a forthcoming paper.

This oscillatory cycle explains the unusual and surprising observation that the oscillations in the H_2O_2–KSCN–$CuSO_4$–NaOH system always appear near the Pt potentials and pHs which are characteristic for SS I, and the periodic change of Pt potential in time resembles the SS I trace superimposed with an oscillatory potential. It also explains the absence of pH oscillations. Owing to the very low conversion of H_2O_2 to H_2O and O_2 per cycle, noticeable oscillations in pH cannot occur at high [OH^-] where the oscillations take place. Oscillations between SS I and SS II predicted by theoretical considerations[17] and found experimentally in many real systems[18] have never been observed in our case. This finding also suggests that the chemistry which determines SS II does not play much role in giving rise to the oscillatory behavior.

Finally, the oscillatory processes in which H_2O_2 participates are summarized in order to emphasize the unique ability of this compound in bringing about exotic chemical phenomena. Periodic reaction and bistability have been found to occur between (i) H_2O_2 and strong oxidants such as IO_3^- in acid medium (Bray reaction);[19]

(9) Fortnum, D. H.; Battaglia, C. J.; Cohen, S. R.; Edwards, J. O. *J. Am. Chem. Soc.* **1960**, *82*, 778–782.
(10) Schumb, W. C.; Satterfield, N. C.; Wentworth, R. L. *Hydrogen Peroxide*; Reinhold: New York, 1955; Chapter 8, pp 447–515.
(11) Barb, W. G.; Baxendale, J. H.; George, P.; Hargrave, K. R. *Trans. Faraday Soc.* **1951**, *47*, 462–500, 591–616.
(12) *Gmelins Handbuch der Anorganischen Chemie*; Sauerstoff, 8. Auflage, Lieferung 7, Wasserstoffperoxid, Verlag Chemie: Weinheim/Bergstr., 1966; p 2290.
(13) Reference 12, pp 2387–2391.
(14) Vierke, G. *Z. Naturforsch., B: Anorg. Chem., Org. Chem.* **1974**, *29*, 135–136.
(15) Glaser, A. *J. Chem. Soc.* **1951**, 904–910.
(16) Cahill, A. E.; Taube, H. *J. Am. Chem. Soc.* **1952**, *74*, 2312–2318.
(17) Boissonade, J.; De Kepper, P. *J. Phys. Chem.* **1980**, *84*, 501–506.
(18) See ref 2, Chapter 7, pp 223–256.

(ii) H_2O_2 and strong reductants such as sulfide[5] and thiosulfate[20] ions in neutral solution without and with catalyst, respectively; and (iii) H_2O_2 and the weak reductant SCN^- with Cu(II) ion present in strong alkaline environment. Although the mechanism of the oscillatory behavior is now understood only for the Bray reaction, it seems safe to state that the chemical background of the periodicity and multistability is rather different in each case.

Acknowledgment. I thank Irving R. Epstein for a critical reading of this manuscript. This work was made possible by a U.S.-Hungarian cooperative grant from the National Science Foundation (INT 8217658) and the Hungarian Academy of Sciences.

Registry No. H_2O_2, 7722-84-1; SCN^-, 302-04-5; Cu, 7440-50-8; NH_4^+, 7664-41-7.

(19) Bray, W. C. *J. Am. Chem. Soc.* **1921**, *43*, 1262-1267.
(20) Orbán, M.; Epstein, I. R., unpublished results.

Conformational Analysis. 10. Ethane-1,2-dithiol. Electron-Diffraction Investigation of the Molecular Structure, Conformational Composition, and Anti-Gauche Energy and Entropy Differences. Evidence for an Intramolecular SH···S Hydrogen Bond

Sarah L. Barkowski, Lise Hedberg, and Kenneth Hedberg*

Contribution from the Department of Chemistry, Oregon State University, Corvallis, Oregon 97331. *Received June 30, 1986*

Abstract: The structure and conformational composition of gaseous ethane-1,2-dithiol have been investigated at nozzle temperatures of 350 and 445 K. The analysis was based on refinements of electron-diffraction data augmented by rotational constants and, in a newly developed method, dipole-moment components from the literature. The most important discovery is that one of the H_S atoms is positioned so as to form a S-H···S hydrogen bond in the gauche form of the molecule with the H···S distance equal to 2.70 (8) Å, about 0.4 Å less than the sum of the van der Waals radii. The mole fractions of the gauche conformer at 350 and 445 K are 0.459 (86) and 0.479 (100), respectively, from which the internal energies of the gauche and anti forms are calculated not to be significantly different ($\Delta E^\circ = E_G^\circ - E_A^\circ$ = 0.41 (86) kcal mol^{-1}) and the entropy difference $\Delta S^\circ = S_G^\circ - S_A^\circ - R \ln 2$ to be −1.0 (22) cal deg^{-1} mol^{-1}. Assuming that the conformers differ only in their C–C and C–S torsion angles, the values of some of the more important parameters at 350 K with 2σ values that include estimates of systematic error and correlations among observations are r_g(C–H) = 1.118 (11) Å, r_g(S–H) = 1.373 (15) Å, r_g(C–C) = 1.537 (6) Å, r_g(C–S) = 1.824 (2) Å, $\angle_\alpha$CCS = 113.1 (4)°, $\angle_\alpha$HCH = 103.7 (57)°, $\angle_\alpha$CCH = 111.1 (13)°, $\angle_\alpha$SCH = 108.8 (13)°, τ(SCCS) = 69.0 (15)°, l(C–H) = 0.086 (8) Å, l(S–H) = 0.090 (8) Å, l(C–C) = 0.054 (5) Å, l(C–S) = 0.059 (3) Å, σ_A(root mean square amplitude of C–C_A torsion) = 14.9 (52)°. The torsion angles CCSH in the gauche form have values equal to −40 (30)° and −141 (22)° measured in the sense of a counterclockwise rotation of the S–H bonds relative to an eclipsed arrangement of these bonds with τ(SCCS) equal to 0.0°. The frequency of the torsional vibration in the anti form of the molecule is calculated from σ_A to be 87 (24) cm^{-1} in good agreement with the experimental value 115 cm^{-1}.

The molecules of 1,2-disubstituted ethanes exist as mixtures of anti and gauche conformers as a result of rotation about the C–C bond. Which of these forms is the more stable for a given substance depends on the relative importance of steric repulsion on the one hand and internal hydrogen bonding and/or the "gauche effect"[1] on the other. Substances that afford the possibility of hydrogen-bond formation, such as ethylenediamine,[2,3] ethylene glycol,[4] 2-fluoroethanol,[5] 2-aminoethanol,[6] 2-mercaptoethanol,[7] and 2-chloroethanol,[8] are found to be 80–99% gauche in the gas at room temperature. In 1,2-difluoroethane where hydrogen-bond formation is not possible but where the gauche effect is presumed to be important, the molecules are found to be about 95% gauche.[9] In the absence of either a strong gauche effect or hydrogen bonding, such as in 1,2-dichloroethane, the anti form predominates (60–90%).

The molecule ethane-1,2-dithiol (hereafter EDT) diagrammed in Figure 1 also poses the possibility of intramolecular hydrogen-bond formation. Although a bond of the type S–H···S in the gauche conformer would surely be weak because of the unfavorable electronegativity of the sulfur atom, bonds—or at least arrangements—of the type S–H···N and O–H···S apparently exist (in 2-aminoethanethiol[10] and 2-mercapoethanol[7]) and show that sulfur may act either as a donor or an acceptor of hydrogen. The structure and composition of EDT at about 70 °C have previously been investigated[11] by electron diffraction, from which it was concluded that the anti form was the more stable by about 0.8

(1) Wolfe, S. *Acc. Chem. Res.* **1972**, *5*, 102.
(2) Yokozeki, A. Kuchitsu, K. *Bull. Chem. Soc. Jpn.* **1971**, *44*, 2926.
(3) Marstokk, K. M.; Møllendal, H. *J. Mol. Struct.* **1978**, *49*, 221.
(4) Caminati, W.; Corbelli, G. *J. Mol. Spectrosc.* **1981**, *90*, 572.
(5) Hagen, K.; Hedberg, K. *J. Am. Chem. Soc.* **1973**, *95*, 8263.
(6) Penn, R. E.; Curl, R. F. *J. Chem. Phys.* **1971**, *55*, 651.
(7) Sung, E.-M.; Harmony, M. D. *J. Am. Chem. Soc.* **1977**, *99*, 5603.
(8) Almenningen, A.; Bastiansen, D.; Fernholt, L.; Hedberg, K. *Acta Chem. Scand.* **1971**, *25*, 1946.
(9) Friesen, D.; Hedberg, K. *J. Am. Chem. Soc.* **1980**, *102*, 3987.
(10) Nandi, R. N.; Boland, M. F.; Harmony, M. D. *J. Mol. Spectrosc.* **1982**, *92*, 419.
(11) Schultz, Gy.; Hargittai, I. *Acta Chim. Acad. Sci. Hung.* **1973**, *75*, 381.

0002-7863/86/1508-6898$01.50/0